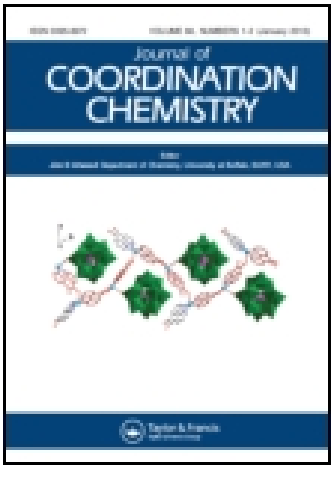

Journal of Coordination Chemistry
Publication details, including instructions for authors and subscription information:
http://www.tandfonline.com/loi/gcoo20

Synthesis, characterization, and DNA binding of two copper(II) complexes as DNA fluorescent probes

Ran-Ran Duan[a], Lu Wang[a], Wei-Qiang Huo[a], Shi Chen[ab] & Xiao-Hua Zhou[ab]

[a] College of Science, South China Agricultural University, Guangzhou, PR China

[b] Institute of Biomaterial, South China Agricultural University, Guangzhou, PR China

Accepted author version posted online: 25 Jul 2014.Published online: 18 Aug 2014.

To cite this article: Ran-Ran Duan, Lu Wang, Wei-Qiang Huo, Shi Chen & Xiao-Hua Zhou (2014) Synthesis, characterization, and DNA binding of two copper(II) complexes as DNA fluorescent probes, Journal of Coordination Chemistry, 67:16, 2765-2782, DOI: 10.1080/00958972.2014.946918

To link to this article: http://dx.doi.org/10.1080/00958972.2014.946918

Journal of Coordination Chemistry, 2014
Vol. 67, No. 16, 2765–2782, http://dx.doi.org/10.1080/00958972.2014.946918

Synthesis, characterization, and DNA binding of two copper (II) complexes as DNA fluorescent probes

RAN-RAN DUAN†, LU WANG†, WEI-QIANG HUO†, SHI CHEN†‡ and XIAO-HUA ZHOU*†‡

†College of Science, South China Agricultural University, Guangzhou, PR China
‡Institute of Biomaterial, South China Agricultural University, Guangzhou, PR China

(*Received 1 January 2014; accepted 4 June 2014*)

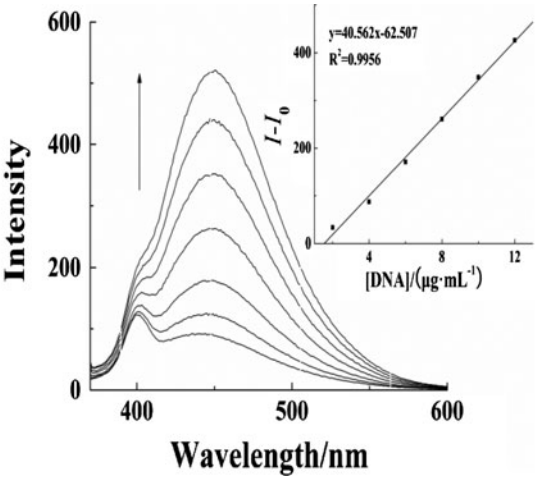

Two copper(II) complexes, $[Cu(DAPT)_2Cl]Cl{\cdot}H_2O$ and [Cu(DBM)(DAPT)Cl] [DAPT = 2,4-diamine-6-(pyrazin-2-yl)-1,3,5-triazine], were synthesized and characterized. The complexes interact with ct-DNA through classical intercalation. Fluorescence intensity changes of **1** and **2** in the absence and presence of ct-DNA have been investigated for quantitative determination of ct-DNA with the limit of detection of 3.8 and 7.7 ng mL^{-1}.

$[Cu(DAPT)_2Cl]Cl{\cdot}H_2O$ and [Cu(DBM)(DAPT)Cl] [DAPT = 2,4-diamine-6-(pyrazin-2-yl)-1,3,5-triazine] were synthesized and characterized by IR and UV spectroscopy, elemental analysis, TG–DTA, molar conductivity, and LC–MS. The interaction with calf thymus DNA (ct-DNA) of the two complexes has been studied using UV spectra, fluorescent spectra, cyclic voltammetry, and viscosity measurements. The complexes interact with ct-DNA through classical intercalation. Fluorescence intensity changes of **1** and **2** in the absence and presence of ct-DNA have been investigated for quantitative determination of ct-DNA with the limit of detection of 3.8 and 7.7 ng mL^{-1}, respectively. From the result, the two complexes are potentially sensitive DNA fluorescent probes.

*Corresponding author. Email: xhzhou@scau.edu.cn

Keywords: 1,3,5-Triazine-2,4-diamine; Copper(II) complex; DNA-binding; Fluorescent probe; DNA detection

Introduction

The interaction of small molecules with DNA is playing a significant role in the study of anticancer medicine, antibacterial pesticides, and DNA fluorescent probes [1–4]. There are three main interactions, covalent binding, cleavage binding, and non-covalent binding which involves electrostatic binding, groove binding, and intercalation binding. DNA molecular fluorescent probes are important in bioinorganic chemistry with the further development of genomics research [5, 6]. More and more small organic molecules or complexes interaction with DNA have been applied to detection of DNA, which makes the high performance fluorescent probes screened, especially with high sensitivity [7]. For example, Zhang *et al.* studied the taurine–salicylaldehyde Schiff base copper(II) complex and the limit of detection (LOD) was 7 ng mL^{-1} for calf thymus DNA (ct-DNA), 3 ng mL^{-1} for yeast DNA and 3 ng mL^{-1} for sm-DNA [8]. Yegorova *et al*. prepared a water-soluble terbium(III) complex that was highly luminescent and did not require luminescence enhancers for determination of DNA [9]. Metal complexes used as DNA fluorescent or optical probes provide important practical and critical value for exploring DNA structure and genetic information, especially the DNA of lesions. They showed potential application prospects in gene therapies and antitumor drugs [10, 11].

2,4-Diamine-6-(pyridine-2-yl)-1,3,5-triazine (DAPT) and its derivatives are pharmaceutical intermediates due to their anticancer and anti-angiogenic activity [12–15]. DAPT has many nitrogens, potential hydrogen-bond acceptors or donors, forming H-bond patterns [16]. If these potential H-bond donors or acceptors occupied the site against DNA base pairs, high sequence-specific non-covalent interactions will exist between DAPT and the DNA grooves [17]. So DAPT performs primarily in identifying and detecting DNA molecules through bonding with DNA. Slinchenko *et al*. have reported that the structure of 4,6-diamino-1,3,5-triazine could recognize the A–T base pairs of ds-DNA [18]. Many substituted-s-triazine compounds have displayed comparable antibacterial activity against *Bacillus sphaericus* and other tested organisms significantly with reference to streptomycin [19].

Dibenzoylmethane (DBM) and its complexes have been widely considered as fluorescent materials and anticancer drugs in biotechnology and pharmaceuticals although DBM is a common β-diketone. For example, Jackson provided new insights into how DBM regulated the androgen receptor (AR) function and cell growth, as well as providing promising evidence to support DBM as a chemotherapeutic agent for prostate cancer through suppression of the function of AR [20]. Thimmulappa *et al*. also indicated that DBM mediated the induction of phase II enzymes by Nrf2 activation and inhibits benzo[a]pyrene-induced DNA adducts by enhancing its detoxification in lungs [21].

DAPT reflects favorable DNA binding and recognition performance, DBM shows desirable luminescence properties and biological activities; if they are used as ligands for coordination compounds, owing to the coordination synergistic effect, more sensitive and higher biological active DNA fluorescence probes could be obtained.

In the present work, two new copper(II) complexes with DBM and DAPT were prepared and characterized. Their ct-DNA binding attributions were investigated. The two complexes combined with ct-DNA by intercalation into base pairs to form a stable complex, which

was confirmed by electronic absorption spectrum, fluorescent spectrum, cyclic voltammetry (CV), and viscosity measurements. They are potential-sensitive DNA fluorescent probes of ct-DNA and quantitative determination reagents.

Experimental

Apparatus and reagents

ct-DNA, ethidium bromide (EB), and Hoechst 32588 were obtained from Sigma Chemicals Co. (USA). Other reagents and solvents of analytical grade were purchased in China. All experiments on interaction with ct-DNA were performed in trishydroxymethylaminomethane (Tris)–HCl buffer which was obtained by mixing 50 mM NaCl with 5 mM Tris in double distilled water and adjusted to pH 7.2 with hydrochloric acid. All ct-DNA solutions were obtained by dissolving to a certain concentration with Tris–HCl buffer to get a ratio of UV absorbance of about 1.8–1.9 at 260 and 280 nm, which indicates no protein and the concentration of ct-DNA was determined according to the molar absorption coefficient 6600 cm^{-1} at 260 nm [22–24]. The complex solutions interacting with ct-DNA were prepared in a mixed solvent of 1% DMF and 99% Tris–HCl buffer.

Elemental analysis (CHN) was performed via an Elemental Vario EL analyzer. The infrared spectrum was obtained through a ACATAR 360 FT-IR spectrophotometer from Nicolet Co. The UV spectrum was carried out on a UV–Vis 2550 spectrophotometer from Shimadzu Co. in Japan. Fluorescence spectra were recorded on a fluorescence photometer (RF-5301PC) of Shimadzu. CV was measured on CHI660E electrochemical workstation. Thermogravimetric analysis was studied on a Shimazdu TG–DTA. ESI-MS was performed on Agilent 6430 M.

Physical measurement

Synthesis of DAPT. DAPT was prepared according to the literature [25] and recrystallized from ethanol. The synthetic reaction is shown in figure 1.

Synthesis of the complexes. *Complex 1*. DAPT (0.376 g, 2 mM) was dissolved in ethanol and then $CuCl_2$ (0.24 g, 1 mM) was added with stirring. Green precipitate was produced when the pH was adjusted to 2.5 with NaOH. The deposit was filtered after 2 h stirring and green crystals were obtained from the filtered solution in two weeks. Yield: 64%.

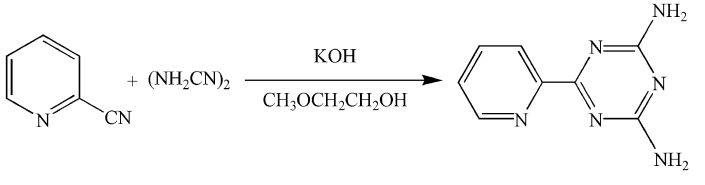

Figure 1. The synthesis of DAPT.

Anal. Calcd for $CuC_{16}H_{18}N_{12}OCl_2$ (%): C, 36.34; H, 3.43; N, 31.78. Found: C, 36.35; H, 3.51; N, 31.41. Λ_m (in CH_3OH): 103.6 S cm^2 mol^{-1}. TG (weight loss, %): Calcd for H_2O, 3.31; Cl, 13.36; DAPT, 69.82. Found: H_2O, 3.41; Cl, 13.43; DAPT, 71.21. IR (cm^{-1}): 3344($\nu^{as}_{NH_2}$); 3176($\nu^{s}_{NH_2}$); 1382, 1401($\nu_{-C=N}$); 1585($\nu_{C=C}$), 1573($\nu_{C=C}$). UV: 280 nm. ESI-MS (*m*/*z*): 474.1 ($[Cu(DAPT)_2Cl]^+$).

Complex ***2***. DAPT (0.188 g, 1 mM) and DBM (0.2242 g, 1 mM) were dissolved in ethanol then $CuCl_2$ (0.24 g, 1 mM) was added with continuous stirring. Precipitate was produced after the pH was adjusted to 3. After filtration green crystals were separated from the mother liquor after two days. Yield: 71%. Anal. Calcd for $CuC_{23}H_{19}O_2N_6Cl$ (%): C, 54.12; H, 3.75; N, 16.46. Found: C, 54.01; H, 3.94; N, 16.43. Λ_m (in CH_3OH): 27.7 S cm^2 mol^{-1}. TG (weight loss, %): Calcd for Cl, 6.94; DBM, 43.33; DAPT, 36.82. Found: Cl, 6.93; DBM, 43.75; DAPT, 36.71. IR (cm^{-1}): 3333($\nu^{as}_{NH_2}$), 3160($\nu^{s}_{NH_2}$), 1678, 1654($\nu_{C=O}$), 1595 ($\nu_{C=C}$), 1450(ν_{C-H}), 1370($\nu_{C=N}$). ESI-MS (*m*/*z*): 474.2 ($[Cu(DBM)(DAPT)]^+$).

DNA binding experiments

UV spectra were recorded by keeping the concentration of the complexes constant when varying the concentration of ct-DNA from 200 to 500 nm ([DNA]/[complex **1**] = 0–3.5, [DNA]/[complex **2**] = 0–0.6). The complex/DNA system was equilibrated for 15 min after the addition of DNA at 25 °C.

Thermal denaturation experiments of ct-DNA were carried out with increasing temperature from 40 to 90 °C at a rate of 1 °C min^{-1} and the UV absorbance was continuously monitored at 260 nm. The data were depicted through relative absorbance *versus* temperature at 260 nm.

The fluorescence intensity of competitive binding experiments was performed by keeping the concentration of ct-DNA (10 μM) and EB (5 μM) fixed while the complexes were gradually added (0–10 μM). The changes in fluorescence intensity were monitored after each addition of the complexes with 15 min equilibration.

Viscosity measurements were carried out on an Ubbelohde viscometer in a thermostatic water bath with constant temperature 29.0 ± 0.1 °C. The complex was added gradually to the solution of ct-DNA (50 μM). The viscosity of the mixed complex/DNA system was measured after 2 h.

In CV, glassy carbon electrode modified by carbon nanotubes as a working electrode, saturated calomel electrode as reference electrode, and counter electrode of platinum electrode constitute the three electrode systems. The ct-DNA was added to the complex solution. The CV curve was recorded after 10 min equilibration. The time of pulse was 0.05 s, the initial potential was −1 V, the termination potential was 1 V, and scanning speed was 50 mV s^{-1}.

The determination of ct-DNA

Four testing conditions, viz. pH of Tris–HCl, concentration of the complex, reaction time, and ionic strength, in DNA determination are discussed. The pH of Tris–HCl was varied from 3 to 13 with fixed concentration ratio of the complex to ct-DNA ([complex] = 10 μg mL^{-1}, [DNA] = 5 μg mL^{-1}). The concentration of DNA was constant ([DNA] = 5 μg mL^{-1}) when the gradual addition of **1** and **2** ranged from 0 to 8 and 0 to 15 μg mL^{-1}, respectively. Effects of ionic strength were measured by the changes in

fluorescence intensity with addition of NaCl ranging from 0 to 70 mM L^{-1} in the complex/DNA systems under the obtained optimization conditions.

The fluorescence emission spectra were recorded through gradual addition of ct-DNA to the complex solutions ([complex **1**] = 4 μg mL^{-1}, [complex **2**] = 6 μg mL^{-1}). The concentrations of **1** and **2** were varied in the range of 0–12 and 0–16 μg mL^{-1}, respectively. Tests for coexisting interference substances were performed by fluorescence intensity changes in the absence and presence of interference substances in the system of the complexes (10 μg mL^{-1}) and DNA (5 μg mL^{-1}).

Results and discussion

Structural characterization of the complexes

UV–vis spectra. The two complex solutions used for UV–vis spectra were obtained by dissolving them in CH_3OH. The absorbances at 210 and 271 nm are assigned to $\pi \rightarrow \pi^*$ transitions of the aromatic ring in DAPT, while 251 and 348 nm are due to the $\pi \rightarrow \pi^*$ transition of the benzene ring and $n \rightarrow \pi^*$ transition of the carbonyl of DBM, respectively. Compared with DAPT and DBM, the absorption peaks of **1** are at 213 and 280 nm and for **2** at 273 and 354 nm, which showed a red shift. The weak and broad d–d* transition of **1** and **2** at 742 and 630 nm correspond to $^2B_{1g} \leftarrow {}^2A_{1g}(d_{x2-y2} \leftarrow d_{z2})$ $v1$ transitions and the spectra are typical of Cu(II) complexes with an elongated tetragonal structure [26, 27].

IR spectra. The band around 3350–3100 cm^{-1} of both complexes was assigned to vibration of the amino groups $\nu^{as}_{NH_2}$ and $\nu^{s}_{NH_2}$. The bands at 1382 and 1401 cm^{-1} for **1** and 1370 cm^{-1} for **2** can be attributed to vibration of the cyano group ($\nu_{-C\equiv N}$). The carbonyl stretching vibration of free DBM is at 1597 cm^{-1}, divided into two peaks at 1591 and 1551 cm^{-1}, which characterize the enolate anion of DBM with coordination [28–30]. Weak peaks at 460 and 522 cm^{-1} were assigned to Cu–N and Cu–O [30–32]. Compared with the ligands, the peaks of the complexes had a shift in wavenumber and changes in absorption strength, which also showed coordination of the ligands to copper(II).

Thermal analysis. Thermal decomposition of the complexes was investigated by TG–DTA. For **1**(a), weight losses could be observed from DTA curves. The first was due to loss of crystal water at 57 °C (Calcd = 3.41%, TG = 3.31%) and one chlorine atom at 70 °C (Calcd = 6.70%; TG = 6.83%), from which we deduce that H_2O and one chloride are in the outer sphere. The second weight loss was from loss of coordinated chlorine at 158 °C (Calcd = 6.70%; TG = 6.83%) The third loss-weight peak was at 490 °C when DAPT decomposed (Calcd = 71.21%; TG = 69.82%). For **2**(b), the first mass loss is from one chlorine atom (Calcd = 6.93%, TG = 6.94%) at 146 °C. The last two loss-weight peaks are due to decomposition of DAPT (Calcd = 36.71%, TG = 36.82%) at 500 °C and DBM (Calcd = 43.75%, TG = 43.33%) at 300 °C. The thermal analysis is consistent with the elemental analysis (EA).

LC–MS analysis. Since the measurement conditions was at the mode of ESI-positive ions, complexes in the cationic form were stable under the measurement condition; all the compounds were ionized and the obtained *m*/*z* results were added a hydrogen. For **1**, hydrogen in the amino was easily lost when heating after protonation of the amino group. Thus, the ion fragment of *m*/*z* 474.1 is assigned to $[Cu(DAPT)_2Cl]^+$ and the mass of 476.1 may be an isotope of **1**. Signals at *m*/*z* 475.1 and 477.1 for $[Cu(DAPT)_2Cl]^+ + H^+$ also exist. For **2**, *m*/*z* 474.2, 476.2 (M−Cl) may be assigned to primary and isotopic peaks of [Cu(DBM)(DAPT)]$^+$ in the MS of **2**.

The molar conductivity in CH_3OH of **1** and **2** was 103.6 $cm^2\ mol^{-1}$ and 27.7 S $cm^2\ mol^{-1}$, respectively, and showed that **1** was a type of 1 : 1 electrolyte, while **2** was a non-electrolyte [33].

Based on the results of EA, UV, IR, TG-DSA, LC–MS, and molar conductivity, the probable configurations of the two complexes are depicted in figure 2.

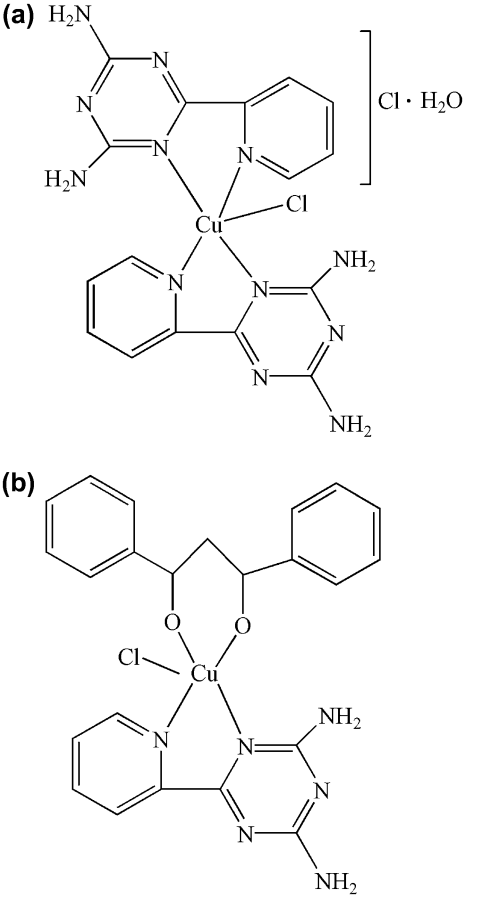

Figure 2. Suggested configuration of **1** (a) and **2** (b).

DNA binding studies

UV spectra. UV absorption titration is a common characterization method in testing the interaction of complexes with DNA through the changes in absorbance and shift in wavelength. It usually shows a certain extent of hypochromism and red shift when a complex binds to DNA through intercalation due to the π–π stacking interaction between the aromatic chromophore and the base pairs of DNA. In this method the DNA binding constant K_b could be calculated by equation (1) [34],

$$[\mathrm{DNA}]/(\varepsilon_a - \varepsilon_f) = [\mathrm{DNA}]/(\varepsilon_b - \varepsilon_f) + 1/K_b(\varepsilon_b - \varepsilon_f) \quad (1)$$

where ε_a is the apparent absorption coefficient $A_{obsd}/[Cu]$, ε_f and ε_b are the extinction coefficients of the free complex and the complex bound to DNA fully, respectively.

Figure 3 shows the absorption spectra of **1**(a) and **2**(b) in the absence and presence of ct-DNA. It is clear that with increasing concentration of DNA, **1** and **2** have a distinct

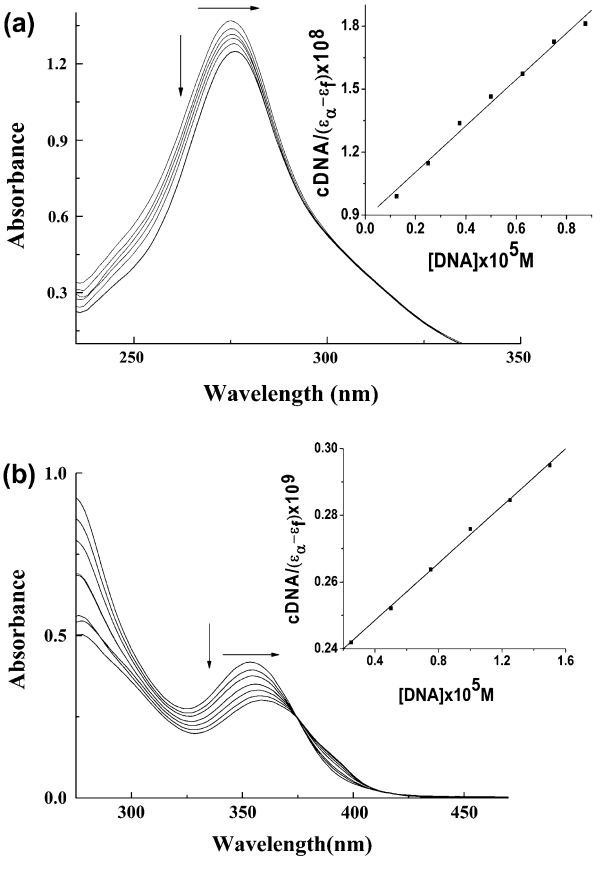

Figure 3. UV spectra of **1** (a) and **2** (b) in Tris–HCl buffer in the presence of increasing amounts of ct-DNA. The arrow indicates the absorbance change upon increasing DNA concentration. $c_{(complex)} = 25$ μM; [DNA]/[complex **1**] = 0, 0.5, 1.0, 1.5, 2.0, 2.5, 3.0, 3.5; [DNA]/[complex **2**] = 0, 0.10, 0.20, 0.30, 0.40, 0.50, 0.6. The insets: the plots of $(\varepsilon_a - \varepsilon_f)/(\varepsilon_b - \varepsilon_f)$ *vs.* [DNA]/[complex] for the titration of DNA to **1** and **2**.

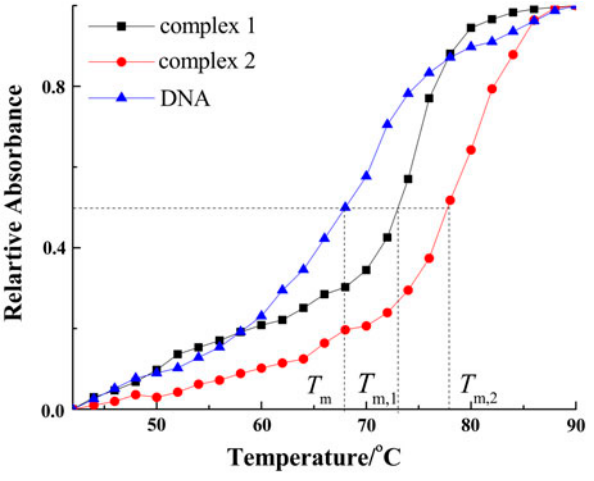

Figure 4. T_m curves of ct-DNA in the absence and presence of **1** or **2**. [DNA] = 70 μM, [complex] = 30 μM.

hypochromism of 8.82%, 30.37% with a red shift of 2 and 5 nm, respectively, which indicates both complexes interact with DNA mainly by intercalation. To compare the DNA binding affinity quantitatively, the binding constants K_b of **1** and **2** were calculated to be 1.1×10^4 and 2×10^4 L mol^{-1}, respectively. DNA affinity of **2** is a little larger than for **1**, mainly due to the second planar ligand DBM.

Thermal denaturation. Thermal denaturation experiments can reflect the configuration change of ct-DNA with increasing temperature and indicate the binding mode of the complexes with DNA. In general, with increasing temperature, the H-bond interaction between DNA base pairs was gradually weakened and ds-DNA dissociated into single strands. The absorbance of purine bases and thymine bases would gradually enhance at 260 nm in the process of chain dissociation [35–37]. The absorbance at 260 nm will steadily increase with temperature when the absorption intensity reached saturation when ds-DNA completely disintegrated into a single strand. Thus, the melting point of DNA (T_m), at which half of ds-DNA dissociated, can reflect the changes in the configuration stability of ct-DNA. The T_m will increase to stabilize the double helix structure of DNA because of the $\pi \rightarrow \pi^*$ accumulation effect when the complexes bind to DNA by intercalation.

The T_m curves of ct-DNA before and after addition of **1** or **2** are given in figure 4. T_m of ct-DNA is changed from 68 to 73 or to 76 °C with addition of **1** and **2**, respectively. However, the ΔT_m ($T_{m,1} - T_m = 5$ °C, $T_{m,2} - T_m = 8$ °C) is comparable to some intercalators but smaller than EB (13 °C) [38]. The increase in T_m indicated that the main interaction of DNA with **1** and **2** is classical intercalation; moreover, **2** has a relatively stronger binding than **1**.

The competitive binding experiments. EB is a conjugated planar molecule with weak fluorescence itself. It can be inserted into the internal base pairs of DNA double helix with

fluorescence enhancement. If the complex that would compete with EB for the DNA-binding site is added into DNA solution, EB will be set free from the double helix of DNA and the fluorescence will reduce significantly, even be quenched [39]. The fluorescence quenching constant K_{sq}, which can be estimated from the extent of intercalation of the complex into DNA, can be obtained quantitatively from equation (2) [38, 40],

$$I_0/I = I + K_{sq}r \tag{2}$$

where I_0 and I are the fluorescence intensity of the complex/DNA system in the absence and presence of **1** and **2**, respectively, and r is the concentration ratio of the complex and DNA. K_{sq} can be obtained from plots of I_0/I *versus* [complex]/[DNA]. As depicted in figure 5, the fluorescence was significantly quenched at the emission peak of 583 nm with addition of **1** and **2** with K_{sq} of 1.73×10^4 and 9.20×10^4, respectively. Complex

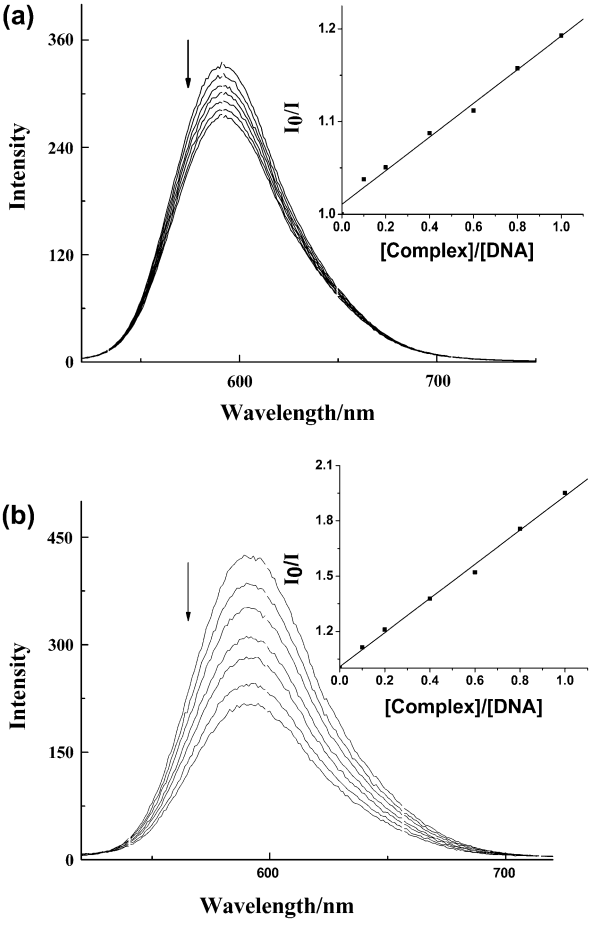

Figure 5. The emission spectra of EB binding to DNA with the presence of **1** (a) and **2** (b) in Tris–HCl buffer solution. [DNA] = 10 μM, [complex] = 0–10 μM.

2 has a stronger quenching constant than **1**, which may be explained by the larger aromatic plane of DBM.

Viscosity measurement. The change in viscosity of ct-DNA solution can reflect the DNA-binding mode after complex addition. A part intercalation of the complex into DNA leads to reduction of the viscosity of the DNA solution [41]. However, a classical intercalation results in lengthening adjacent distance of DNA base pairs to accommodate the inserted ligand and lead the longer DNA double helix to adjust to the ligand intercalation, so that the viscosity will correspondingly increase. In addition, the viscosity of the DNA solution has no obvious change if the complexes interact with DNA by electrostatic or groove binding [42–44].

Figure 6 indicates the effect of EB, Hoechst 33258, and the two complexes on the relative viscosity of ct-DNA. EB, a well-known DNA intercalator, could strongly insert into the internal of DNA and cause the relative viscosity of DNA to increase. Hoechst 33258 is well known as DNA groove agent that could bind to the minor groove of ds-DNA [45]. Different from Hoechst 33258, the effect of **1** and **2** on the viscosity of ct-DNA was similar with that of EB. It can thus be deduced that both the complexes bind to DNA by intercalation. According to the changing trends of relative viscosity of DNA with compound addition, the DNA intercalating potential followed the order EB > **2** > **1**.

CV measurement. Electrochemical methods play an important role in the study of medical molecules interacting with DNA. Because a biological system is usually full of electrolyte solution, a series of processes of pharmacological activities (redox properties) are associated closely to electron transfer in the body. CV is one of the effective means of DNA research because of its sensitivity and high selectivity. The electrolyte binding to the DNA of the complex resulted in negative shift of the redox peak; however, intercalation leads to positive

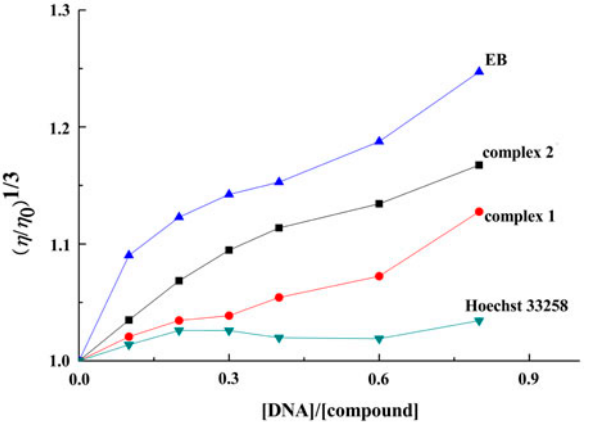

Figure 6. The effect of increasing amounts of EB, **1**, **2** and Hoechst 33258 (from top to bottom, respectively) on the relative viscosity of ct-DNA at 25 °C. [DNA] = 0.1 mM.

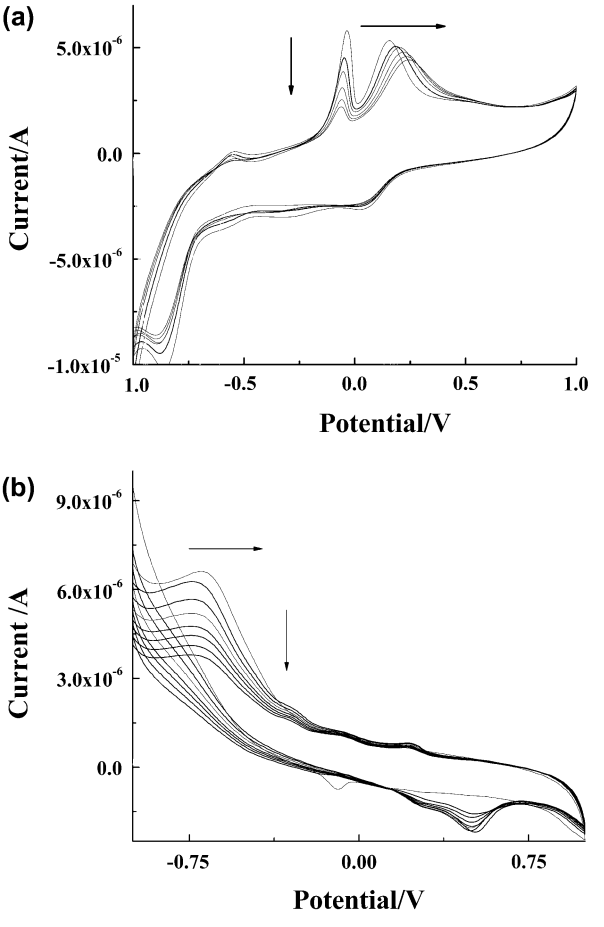

Figure 7. CV curves of **1** (a) and **2** (b) (50 μM) in Tris–HCl buffer solution in the presence of ct-DNA (5, 10, 20, 30, 40, 50 μM); scan rate: 50 mV s^{-1}.

shift [46]. Figure 7 shows the CV curves for **1** and **2** in Tris–HCl buffer solution (pH 7.2) without and with increasing concentrations of ct-DNA.

The voltammetric behavior of both complexes is mainly reduction peaks. The reduction peak potential of **1** was 0.1523 and −0.0363 V; however, the reduction peak of **2** was −0.683 V. The CV curve reveals that the current value decreased for both complexes with a positive shift, which can indicate that the complexes interact with DNA mainly by classical intercalation [47]. This conclusion is consistent with the results obtained above.

Determination of DNA

Optimization of measurement conditions. The preliminary result above indicated that the fluorescence intensity of the complexes enhanced with addition of ct-DNA. The measurement conditions, the pH of buffer solution [figure 8(a)] and the concentration of complexes

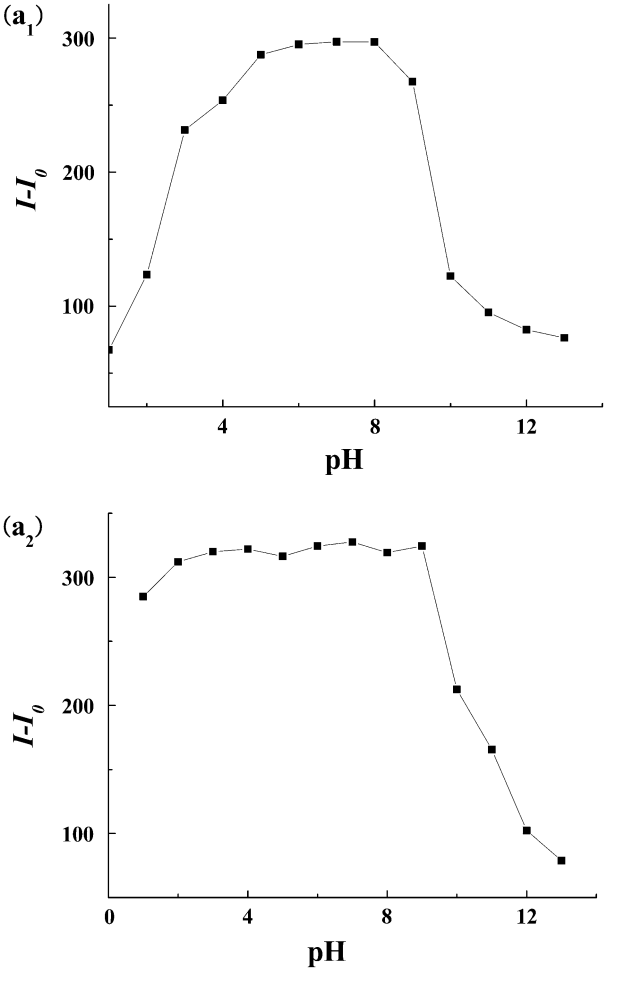

Figure 8. Effects and optimization of measurement conditions. (a) Effects of buffer pH of **1** and **2**. (b) Effects of the complexes concentration, [DNA] = 5 μg mL^{-1}. (c) Effects of [NaCl] on the fluorescence intensities of the complex/ct-DNA systems. [Complex **1**] = 4 μg mL^{-1}, [complex **2**] = 6 μg mL^{-1}; [ct-DNA] = 5 μg mL^{-1}.

[figure 8(b)], were investigated. For pH, it was found that pH ranges of 5–8 and 3–9 for **1** and **2**, respectively, were suitable and 7.2 was used in the experiment in consideration of the simulation of the DNA existent environment. Figure 8(b) gives the changes in fluorescent intensity with increasing concentration of the complexes in DNA solution, and the optimal concentration is 4 and 6 μg mL^{-1} for **1** and **2**, respectively. The reaction time of the complexes with DNA was also considered at room temperature and 5 min was adequate to establish equilibrium.

Effect of the ionic strength in solution. The fluorescence change of the complex/DNA system is shown in figure 8(c) for addition of NaCl. Generally, the fluorescence intensity will weaken with increasing concentration of Na^+ when the complexes interact with DNA through outside binding via electrostatic interaction [45, 48]. Since cations such as Na^+ can

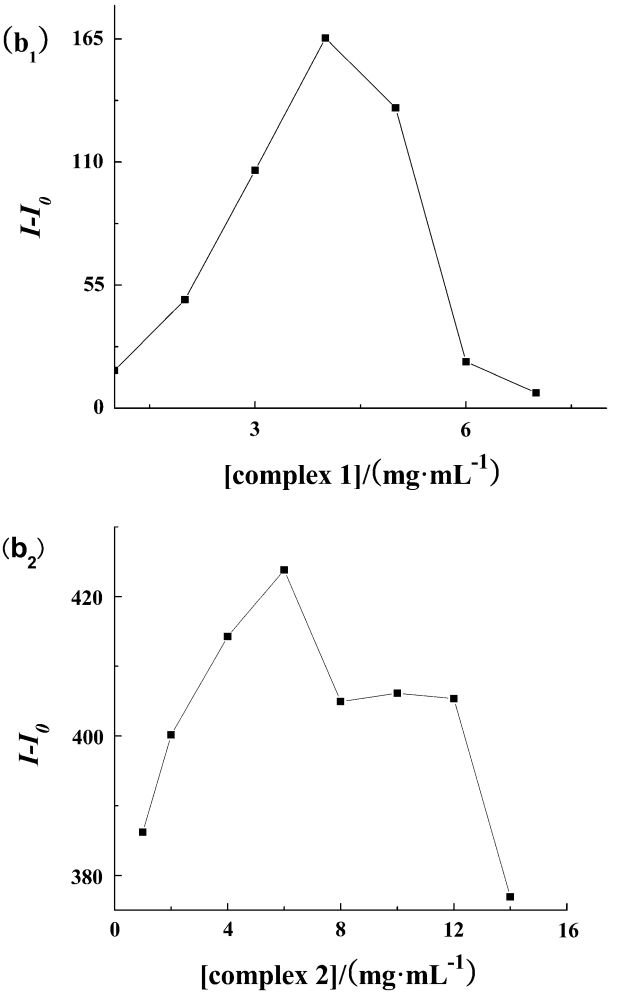

Figure 8. (*Continued*).

bind with negatively charged phosphate groups of DNA through electrostatic interaction, the complex-DNA system will present a degree of fluorescence quenching due to competition with complexes of increasing Na^+ if the complexes interacted with DNA through external electrostatic interaction.

From figure 8(c) the effect of ionic strength on the two complex/DNA systems was different. For **1**, there was no obvious impact, whereas for **2**, the fluorescence had a little enhancement with gradual addition of NaCl. The fluorescence was not quenched with the presence of Na^+ and the outside electrostatic interaction between the complexes and DNA was excluded.

Calibration curves for DNA. The fluorescence spectra of **1** and **2** with different amounts of ct-DNA are given in figure 9. The fluorescence intensity was significantly enhanced

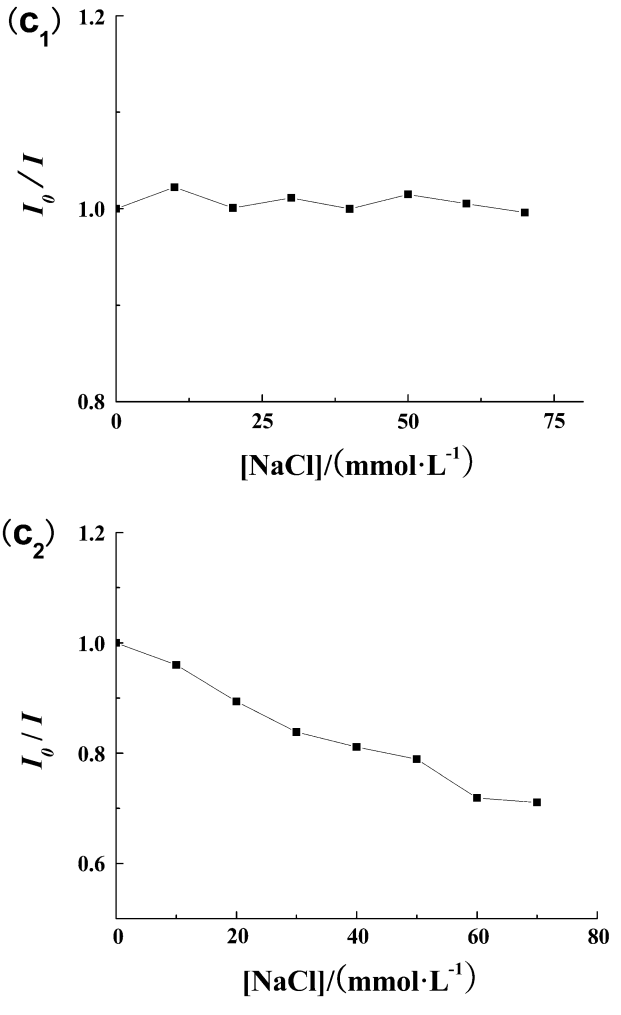

Figure 8. (*Continued*).

when [DNA] increased, exhibiting a good linear relationship between [DNA] and variation of the fluorescence intensity. LOD of **1** and **2** was calculated with equation (3),

$$\mathrm{LOD} = 3S_b/s \tag{3}$$

where S_b is the standard deviation of the blank measurement ($n = 8$) and s is the calibration curves' sensitivity. The linear range in this method was 2–12 and 2–14 μg mL^{-1} for **1** and **2**, respectively. The LOD of **1** and **2** were 3.8 and 7.7 ng mL^{-1}, respectively. The sensitivity of our method was higher than many probes. Comparison of selected luminescence probes for nucleic acid determination is listed in table 1.

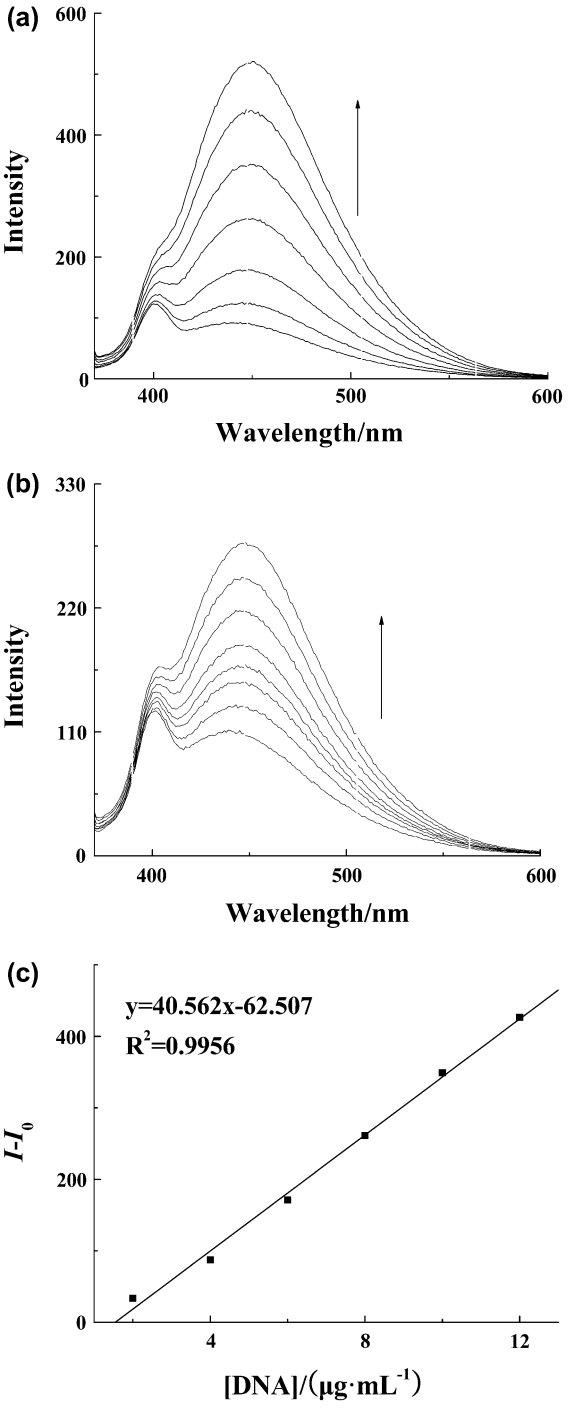

Figure 9. The fluorescence emission spectra of the complex/DNA system at different ct-DNA concentrations. [DNA] = 0, 2, 4, 6, 8, 12, 14 μg mL^{-1}. (a) [Complex **1**] = 4 μg mL^{-1}; (b) [complex **2**] = 6 μg mL^{-1}; (c) and (d) the calibration curves for ct-DNA.

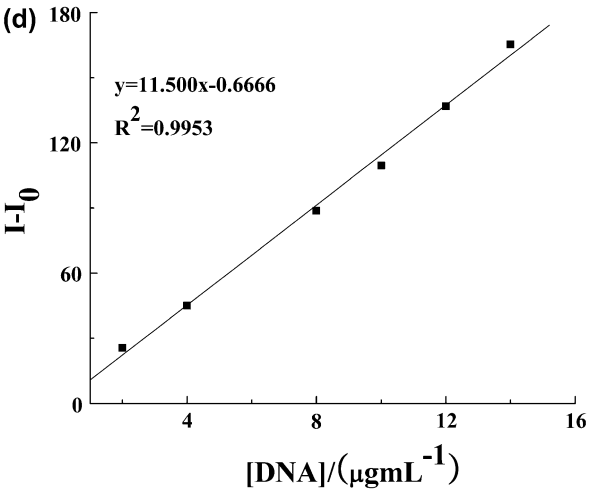

Figure 9. (*Continued*).

Table 1. Comparison of fluorescent probes for DNA detection.

Probe	Linear range (μg mL^{-1})	LOD (ng mL^{-1})	References
EB	–	10	[49]
Eu-benzoylacetone-TAM	0.003–1	0.33, 0.99	[50]
Tb(III)-phenanthroline	0.4–15	100	[51]
Cu-TSSB	0.03–9.03	7	[52]
m-BPO	1.5–15	3.6	[53]
Hoechst 33258	0.25–2	10	[54]
YOYO	0.0005–0.1	0.5	[55]
1	2–12	3.8	This article
2	2–14	7.7	This article

Table 2. Tests for coexisting interference substances in the complexes (10 μM L^{-1}) with DNA (10 μM L^{-1}).

		Changes of fluorescent intensity (%)	
Coexisting substances	Concentration (μM L^{-1})	**1**	**2**
K^+	10	1.67	1.22
Ca^{2+}	10	3.33	3.09
NH_4^+	10	4.21	3.65
Cr^{3+}	10	0.75	2.61
Mn^{2+}	10	2.08	2.15
Co^{2+}	10	8.89	0.83
Ni^{2+}	10	2.56	1.50
Glucose	15	1.77	0.68
Arginine	15	1.16	0.58
Citrate	15	2.39	0.095

Interference of foreign substances. In the DNA detecting environment, there are many coexisting substances. The change of fluorescence intensity was tested with the addition of coexisting substances, such as some common ions, glucose, citrate and amino acid, into the complexes/DNA systems. The effect of coexisting substance on the fluorescent intensity is shown in table 2.

Conclusion

Two new copper(II) complexes including DAPT were synthesized and used as DNA fluorescent probes. The ct-DNA interaction mechanism of the complexes was studied via various methods. The results suggest that the two complexes interact with ct-DNA by classical intercalation, and the DNA affinity of **1** is a little higher than **2**. The two complexes can be used for the detection of ct-DNA with high sensitivity. The LODs of **1** and **2** are 3.84 and 7.7 ng mL^{-1}, respectively. This work will greatly help to understand the mechanism of the complex interaction with DNA and find new fluorescence probes for detecting DNA.

Acknowledgements

The authors are grateful to the Natural Science Foundation of Guangdong, the 211 Project Program Foundation of South China Agricultural University, and the Program of Guangdong Provincial Science & Technology for their financial support.

Supplemental data

The infrared spectra, the TG–DTA curves, LC–MS spectra of complexes figures, and the absorbance spectra table are presented and those can be accessed here http://dx.doi.org/10.1080/00958972.2014.946918.

References

[1] J.L. Yao, X. Gao, W. Sun, S. Shi, T.M. Yao. *Dalton Trans.*, 5661 (2013).
[2] S. Dawson, J.P. Malkinson, D. Paumier, M. Searcey. *Nat. Prod. Rep.*, **24**, 109 (2007).
[3] R.J. Fiel, T.A. Beerman, E.H. Mark, N. Datta-Gupta. *Biochem. Biophys. Res. Commun.*, **107**, 1067 (1982).
[4] M.A. Sari, J.P. Battioni, D. Dupre, D. Mansuy, J.B. Le Pecq. *Biochemistry*, **29**, 4205 (1990).
[5] P.H. Vary, P.R. Andersen, E. Green, J. Hermon-Taylor, J.J. McFadden. *J. Clin. Microbiol.*, **28**, 933 (1990).
[6] E.F. Gudgin Dickson, A. Pollak, E.P. Diamandis. *Pharmacol. Ther.*, **66**, 207 (1995).
[7] L. Li, X. Gao, B. Lv, Z. Zhou, D. Xiao. *Sensor Lett.*, **5**, 441 (2007).
[8] X. Zhang, Y. Wang, Q. Zhang, Z. Yang. *Spectrochim. Acta, Part A*, **77**, 1 (2010).
[9] A. Yegorova, A. Karasyov, A. Duerkop, I. Ukrainets, V. Antonovich. *Spectrochim. Acta, Part A*, **61**, 109 (2005).
[10] J.G. Liu, B.H. Ye, H. Chao, Q.X. Zhen, L.N. Ji. *Chem. Lett.*, **10**, 1085 (1999).
[11] F. Chen, X.P. Ai, Z.K. He, M.J. Li, X.D. Chen. *Spectrosc. Lett.*, **38**, 99 (2005).
[12] P. Gamez, P. de Hoog, M. Lutz, A.L. Spek, J. Reedijk. *Inorg. Chim. Acta*, **351**, 319 (2003).
[13] H. Asanuma, T. Ban, S. Gotoh, T. Hishiya, M. Komiyama. *Supramol. Sci.*, **5**, 405 (1998).
[14] Y. Chen, W. Xu, J. Kou, B. Yu, X. Wei, H. Chao, L. Ji. *Inorg. Chem. Commun.*, **13**, 1140 (2010).
[15] X. Chen, P. Zhan, X. Liu, Z. Cheng, C. Meng, S. Shao, C. Pannecouque, E.D. Clercq, X. Liu. *Bioorg. Med. Chem.*, **20**, 3856 (2012).
[16] K.E. Maly, E. Gagnon, T. Maris, J.D. Wuest. *J. Am. Chem. Soc.*, **129**, 4306 (2007).

[17] P. Uma Maheswari, M. Palaniandavar. *J. Inorg. Biochem.*, **98**, 219 (2004).
[18] O. Slinchenko, A. Rachkov, H. Miyachi, M. Ogiso, N. Minoura. *Biosens. Bioelectron.*, **20**, 1091 (2004).
[19] Y. Zhou, C. Chow, D.E. Murphy, Z. Sun, T. Bertolini, J.M. Froelich, S.E. Webber, T. Hermann, D. Wall. *Bioorg. Med. Chem. Lett.*, **18**, 3369 (2008).
[20] K.M. Jackson, M.C. Frazier, W.B. Harris. *Anticancer Res.*, **27**, 1483 (2007).
[21] R.K. Thimmulappa, T. Rangasamy, J. Alam, S. Biswal. *Med. Chem.*, **4**, 473 (2008).
[22] J. Marmur, P. Doty. *J. Mol. Biol.*, **3**, 585 (1961).
[23] V.A.R. Huss, H. Festl, K.H. Schleifer. *Syst. Appl. Microbiol.*, **4**, 184 (1983).
[24] A.W. Ravin, V.N. Iyer. *J. Gen. Microbiol.*, **26**, 277 (1961).
[25] F.H. Case. *J. Heterocycl. Chem.*, **5**, 223 (1968).
[26] S. Chandra, D. Jain, A.K. Sharma, P. Sharma. *Molecules*, **14**, 174 (2009).
[27] R.G. McDonald, M.J. Riley, M.A. Hitchman. *Inorg. Chem.*, **27**, 894 (1988).
[28] B. Yan, H. Zhang, S. Wang, J. Ni. *Mater. Chem. Phys.*, **51**, 92 (1997).
[29] Z. Bian, K. Wang, L. Jin. *Polyhedron*, **21**, 313 (2002).
[30] F.T. Wall, W.F. Claussen. *J. Am. Chem. Soc.*, **61**, 2812 (1939).
[31] J.R. Ferraro, W.R. Walker. *Inorg. Chem.*, **4**, 1382 (1965).
[32] E.J. Baran, B.S. Parajón-Costa, T. Rojo, R. Sáez-Puche, F. Fernández, R.M. Tótaro, M.C. Apella, S.B. Etcheverry, M.H. Torre. *J. Inorg. Biochem.*, **58**, 279 (1995).
[33] W.J. Geary. *Coord. Chem. Rev.*, **7**, 81 (1971).
[34] A. Wolfe, G.H. Shimer, T. Meehan. *Biochemistry*, **26**, 6392 (1987).
[35] E. Tselepi-Kalouli, N. Katsaros. *J. Inorg. Biochem.*, **37**, 271 (1989).
[36] P.U. Maheswari, V. Rajendiran, M. Palaniandavar, R. Parthasarathi, V. Subramanian. *J. Inorg. Biochem.*, **100**, 3 (2006).
[37] M. Cory, D.D. McKee, J. Kagan, D.W. Henry, J.A. Miller. *J. Am. Chem. Soc.*, **107**, 2528 (1985).
[38] C.V. Kumar, J.K. Barton, N.J. Turro. *J. Am. Chem. Soc.*, **107**, 5518 (1985).
[39] J.R. Lakowicz, G. Weber. *Biochemistry*, **12**, 4171 (1973).
[40] J.M. Kelly, A.B. Tossi, D.J. McConnell, C. OhUigin. *Nucleic Acids Res.*, **13**, 6017 (1985).
[41] G. Cohen, H. Eisenberg. *Biopolymers*, **8**, 45 (1969).
[42] S. Satyanarayana, J.C. Dabrowiak, J.B. Chaires. *Biochemistry*, **31**, 9319 (1992).
[43] P. Lincoln, B. Nordén. *J. Phys. Chem. B*, **102**, 9583 (1998).
[44] K. Bielawski, A. Bielawska, T. Anchim, S. Wolczynski. *Biol. Pharm. Bull.*, **28**, 1004 (2005).
[45] S.C.M. Gandini, V.E. Yushmanov, J.R. Perussi, M. Tabak, I.E. Borissevitch. *J. Inorg. Biochem.*, **73**, 35 (1999).
[46] M.T. Carter, A.J. Bard. *J. Am. Chem. Soc.*, **109**, 7528 (1987).
[47] M.T. Carter, M. Rodriguez, A.J. Bard. *J. Am. Chem. Soc.*, **111**, 8901 (1989).
[48] M.T. Record Jr., T.M. Lohman, P.D. Haseth. *J. Mol. Biol.*, **107**, 145 (1976).
[49] J.B. Le Pecq, C. Paoletti. *Anal. Biochem.*, **17**, 100 (1966).
[50] X. Wu, Ch. Guo, J. Yang, M. Wang, Y. Chen, J. Liu. *J. Fluoresc.*, **15**, 655 (2005).
[51] D. Janovska, F. Vymola, T. Godova. *J. Hyg. Epidemiol. Microbiol. Immunol.*, **28**, 33 (1984).
[52] X. Zhang, Y. Wang, Q. Zhang, Z. Yang. *Spectrochim. Acta, Part A*, **77**, 1 (2010).
[53] B. Qiu, L. Guo, W. Wang, G. Chen. *Biosens. Bioelectron.*, **22**, 2629 (2007).
[54] C. Labarca, K. Paigen. *Anal. Biochem.*, **102**, 344 (1980).
[55] H.S. Rye, J.M. Dabora, M.A. Quesada, R.A. Mathies, A.N. Glazer. *Anal. Biochem.*, **208**, 144 (1993).